One- and two-proton transfer reactions in $^{32}S + ^{64}Ni$ and $^{28}Si + ^{68}Zn$ at near-barrier energies

S. Saha,* Y. K. Agarwal, and C. V. K. Baba
Tata Institute of Fundamental Research, Bombay 400005, India
(Received 14 June 1993; revised manuscript received 17 January 1994)

One- and two-proton transfer reactions were studied at bombarding energies around the barrier in $^{32}S + ^{64}Ni$ and $^{28}Si + ^{68}Zn$ systems. The decrease of one- and two-proton stripping probabilities with the distance of closest approach was observed to be slower than that expected from semiclassical considerations, at above barrier energies, especially for two-proton stripping. The effect of these transfer channels on the sub-barrier fusion enhancement was investigated on the basis of semiclassical theories. It was found that the couplings to the inelastic channels and the one- and two-proton transfer channels cannot explain the observed enhancement, indicating the importance of the one- and two-neutron transfer channels in explaining the fusion data.

PACS number(s): 25.70.Hi, 25.70.Bc, 25.70.Jj

I. INTRODUCTION

There are extensive data on the heavy ion fusion cross sections for energies around the Coulomb barrier [1]. The most pertinent result of these studies is the enhancement of fusion cross sections over those expected on the basis of one-dimensional tunneling through the barrier, known as the one-dimensional barrier penetration model (OBPM), a phenomenon observed for many systems where the product of the atomic numbers of the projectile and the target nuclei is more than ~ 200. A related observation is the broadening of the angular momentum distribution in comparison to the OBPM prediction. There have been several attempts to explain these features [2–7]. The most commonly used prescription for the coupled channels approach to fusion is that due to Dasso, Landowne, and Winther [7] incorporated into the code CCFUS [8]. In such calculations, the coupling due to the inelastic excitation to the collective quadrupole and octupole modes of both the target and the projectile, together with the few nucleon transfer channels, can be included. The relevant form factors for the inelastic couplings are taken as the sum of Coulomb and nuclear inelastic form factors. The data on the transfer form factors are, however, not available in many cases. As a result, in most of the existing analyses of the experimental data only the inelastic channels are coupled. Such analyses account only partly for the observed enhancement of the fusion cross sections below the barrier. The isotopic differences of fusion enhancements in $^{58}Ni + ^{58,64}Ni$ [9] and $^{32,36}S + ^{58,64}Ni$ [10] also indicate the importance of inclusion of the transfer channels in the calculations. Often, the enhancement of the cross section over the OBPM prediction is expressed in terms of the barrier shift D_0, which is the difference between the energy where the experimental or calculated fusion cross section assumes a given small value (here taken as 0.1 mb) and the energy where the OBPM predicts the same cross section.

Calculation of the transfer form factors is possible following the semiclassical approach of Broglia, Pollarolo, and Winther [11] in a limited number of nuclei near the shell closure. A few experimental attempts to include the transfer couplings have been made. Corradi *et al.* [12] studied various transfer reactions in the $^{33}S + ^{90,91,92}Zr$ systems at two energies around the Coulomb barrier. Using a simplified semiclassical approach, they extrapolated the small angle (corresponding to large distances of closest approach) data on the basis of an expected functional form of the form factor and used these form factors in the CCFUS calculations. The barrier shifts so calculated agreed reasonably well with the experiment. They further found that the observed cross sections in multiparticle transfers at large angles (small distances of closest approach) was smaller than the value extrapolated from the small angle data and they attributed this missing cross sections as leading to fusion and thus speculate that the multinucleon transfers may be doorways to fusion.

The study of heavy ion transfer reactions, in itself, is of interest [13,14]. For energies in the region of the barrier, the reactions can be described by the semiclassical theories [15,16]. However, in several cases, deviations from the expected behavior were observed [17,18], particularly for two-nucleon transfer reactions. The angular distribution, which in the semiclassical theory can be transformed to the dependence of the transfer probability on the distance of closest approach, showed anomalous behavior giving rise to the so-called "slope anomaly." It has been suggested [17] that the anomaly can be attributed to the inapplicability of the semiclassical theory and one must consider the quantal diffractive effects.

In an earlier work, Dasgupta *et al.* [19] studied the fusion excitation functions and average angular momenta in $^{32}S + ^{64}Ni$ and $^{28}Si + ^{68}Zn$ systems. Stefanini *et al.* [10] and Tighe *et al.* [20] also measured the fusion cross

*Present address: Saha Institute of Nuclear Physics, Calcutta 700 064, India.

sections in ^{32}S + ^{64}Ni. The CCFUS calculations, performed in Ref. [19], including only the inelastic channel couplings, did not fully explain the enhancement over the OBPM prediction, indicating the need to include transfer channels. Stefanini *et al.* [21] also studied transfer reactions in ^{32}S + ^{64}Ni. Including the transfer couplings through effective inelastic form factors in the code PTOLEMY [22], they could achieve a reasonable fit to the existing fusion data. The present work describes an experimental investigation of the charged particle transfer reactions in ^{32}S + ^{64}Ni at two energies above the barrier and in ^{28}Si + ^{68}Zn at six different energies near the barrier. The ground state Q values of up to four-nucleon transfer channels in these two systems are listed in Table I. As can be seen from the table, proton pickup ($+1p$, $+2p$) and neutron stripping ($-1n, -2n$) channels have large negative Q values and perhaps do not contribute significantly to the coupled channels calculations. Section II of this paper describes the experimental details and the results. The semiclassical theory used to analyze the data is highlighted in Sec. III A and the transfer probabilities observed are compared with the theoretical predictions in Sec. III B. The effect of the measured one- and two-proton transfer probabilities on the sub-barrier fusion enhancement is studied in Sec. III C on the basis of CCFUS, where it is shown that inclusion of one- and two-proton transfer channels does not explain the enhancement of the sub-barrier fusion cross sections.

II. EXPERIMENTAL DETAILS AND RESULTS

Beams of ^{28}Si and ^{32}S in the energy range of 80–115 MeV were obtained from the BARC-TIFR 14UD Pelletron Accelerator facility in Bombay. The targets used were ^{64}Ni ($\sim$ 98% enriched) and ^{68}Zn ($\sim$ 97% enriched) of 50 μg/cm^2 and 125 μg/cm^2 thicknesses, evaporated on 25 μg/cm^2 thick carbon backing. The scattered heavy ions were detected over 32°–57° laboratory angles at all energies (83, 90, 95, 100, 110, and 115 MeV) in the ^{28}Si + ^{68}Zn system, at 100 and 110 MeV in the ^{32}S + ^{64}Ni system, and in addition, over 70°–80° at 100 MeV in the latter system, by a one-dimensional position sensitive parallel grid avalanche counter (PS-PGAC) with an angular resolution of about 0.5°. The PS-PGAC with an angular acceptance of 30° was followed by a large area Bragg curve spectroscopy (BCS) detector with nearly the same angular acceptance. This was used to determine the energy (E) and the atomic number (Z) of the scattered ions along with the scattering angle ($\theta_{\rm lab}$) information from the PS-PGAC. A detailed description of the detectors in the above setup is given elsewhere [23]. During most of the experiment, the detector system was placed with its axis at a fixed angle of 45° upstream to cover 32°–57° laboratory angles. During one experimental run in the ^{32}S + ^{64}Ni system, the detector was placed at 75° upstream with an opening angle of 10° to cover 70°–80° laboratory angles.

A two-dimensional plot of the energy of the detected ions and height of the Bragg peak which scales with Z of the ions is shown in Fig. 1. The bands corresponding mostly to one-proton stripping and two-proton stripping are clearly seen. The Z resolution of the BCS detector $\Delta Z/Z$ was about 1/35 for Z = 10–18 and the energy resolution was about 1.6% full width at half maximum (FWHM) for energies in the range of 30–100 MeV. The count rate handling capability of the BCS detector was limited by the large drift time ($\sim$8–10 μs) of the electrons in the 22 cm drift space of the BCS detector. The beam current was therefore limited to about 2–4 particles nA to eliminate the possibility of pulse pileup. No attempt was made to measure the absolute cross sections and only the transfer probabilities [see Eq. (7) for definition] were measured in the present experiment.

Identification of heavy ions by the BCS detector is limited to Z of the ions. The mass number (A) is normally identified from a time-of-flight (TOF) measurement and the energy of the ions. Since we did not have such a system, we have attempted to identify the mass number of the ions by detecting the characteristic γ rays in coincidence with the heavy ions. Two 15 cm×15 cm hexagonal NaI(Tl) detectors, placed at ±90° with respect to the axis of the BCS detector, were used for this purpose. Although the energy resolution of a NaI(Tl) detector is much worse compared to HPGe detectors which are routinely used in larger arrays in such particle-γ coincidence experiments [24], we have used the NaI(Tl) detectors because of higher efficiency. Further, the relatively large level spacing in this mass region results in cleaner coincidence γ-ray spectra compared to those for higher mass regions with smaller level spacings. The advantage of recording the particle-γ coincidence spectra in this situation is that one can resolve the population of the low-lying levels in both the inelastic and transfer channels.

TABLE I. The ground state Q values ($Q_{\rm g.s.}$) of up to four-nucleon transfer channels in the two systems studied in this experiment. See text for nomenclature used for the transfer channels.

System	Channel	$Q_{\rm g.s.}$ (MeV)	Channel	$Q_{\rm g.s.}$ (MeV)	Channel	$Q_{\rm g.s.}$ (MeV)	Channel	$Q_{\rm g.s.}$ (MeV)
^{32}S	$-1p$	−1.41	$-2p$	0.22	$-1p1n$	−6.65	$-2p1n$	−3.34
+ ^{64}Ni	$+1p$	−10.27	$+2p$	−15.83	$+1p1n$	−7.25	$+2p1n$	−11.15
	$-1n$	−8.94	$-2n$	−13.02	$-1p2n$	−8.86	$-2p2n$	−1.62
	$+1n$	−1.02	$+2n$	3.56	$+1p2n$	−1.20	$+2p2n$	−1.48
^{28}Si	$-1p$	−4.98	$-2p$	−4.72	$-1p1n$	−10.38	$-2p1n$	−8.40
+ ^{68}Zn	$+1p$	−7.24	$+2p$	−11.41	$+1p1n$	−5.04	$+2p1n$	−7.33
	$-1n$	−10.70	$-2n$	−14.79	$-1p2n$	−12.44	$-2p2n$	−4.98
	$+1n$	−1.72	$+2n$	1.83	$+1p2n$	0.20	$+2p2n$	1.62

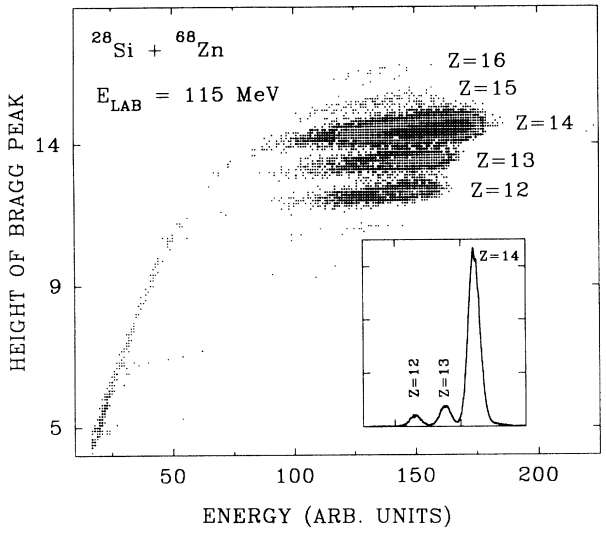

FIG. 1. Two-dimensional plot of Z and E of the ions integrated over the observed angular range in ^{28}Si + ^{68}Zn. Small yields of $Z = 15$ and $Z = 16$ can be seen but were not analyzed. Inset shows E gated Z spectrum.

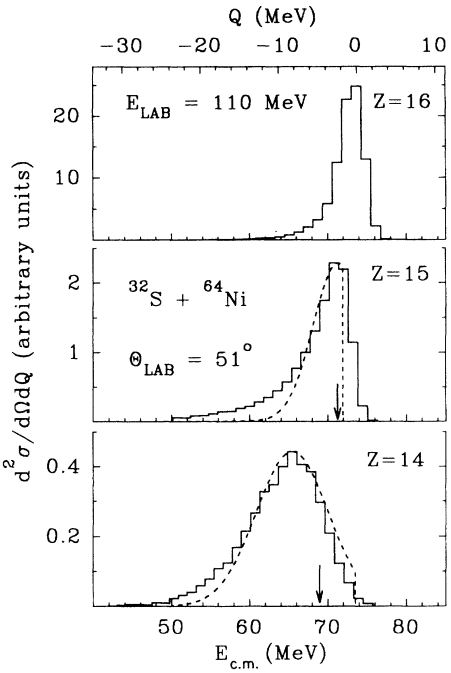

FIG. 2. Q spectra of one- and two-proton stripping at one angle in the ^{32}S + ^{64}Ni system. The dashed lines show the fitted Gaussians between $Q_{g.s.}$ and $-\infty$. The optimum Q values are indicated by the arrows.

This advantage can be utilized to correct the observed particle energy spectra for a given nucleus for contributions from other nuclei with the same atomic number.

The coincidence data, with the master gate generated by the prompt coincidence between the PS-PGAC and either of the two NaI(Tl) detectors, were recorded event by event for off-line analysis. Three-parameter (E, Z, θ_{lab}) singles spectra were simultaneously recorded. From the three-parameter singles data, the energy spectra were sorted out for each Z at ten different θ_{lab}, each with a width of $\sim 2.5°$, covering the angular range of the PS-PGAC. The data at one extreme angle were not considered due to the edge effect.

The energy spectra for the three major Z bands as in Fig. 1, after correction for the energy losses in the foils and the dead layers in the detector, were converted to Q spectra at the corresponding center-of-mass (c.m.) angles. In converting the laboratory energies and angles into the corresponding c.m. quantities, the projectile and the target mass numbers for the Z band in the two-dimensional E-Z spectra corresponding to the incident channel designated by Z_P for the projectile were taken as that for the incident channel, viz., A_P for the projectile and A_T for the target. The mass number of the projectilelike nucleus in the $Z_P - 1$ band was taken as $A_P - 1$ and that in the $Z_P - 2$ band as $A_P - 2$. This is not strictly true because, for example, the Z_P band consists of the neutron transfer channels as well. This, however, introduces only a small error in the c.m. energy and angle. A typical set of Q spectra obtained for the three major Z bands in ^{32}S + ^{64}Ni is shown in Fig. 2.

The coincident γ-ray spectra, gated by the three Z bands in one of the two systems studied, are shown in Fig. 3. An analysis of these γ spectra and similar ones for the ^{28}Si + ^{68}Zn system showed the following features: (i) The γ-ray spectra corresponding to $Z = Z_P$ clearly show the γ rays from the decay of the 2^+ states in both

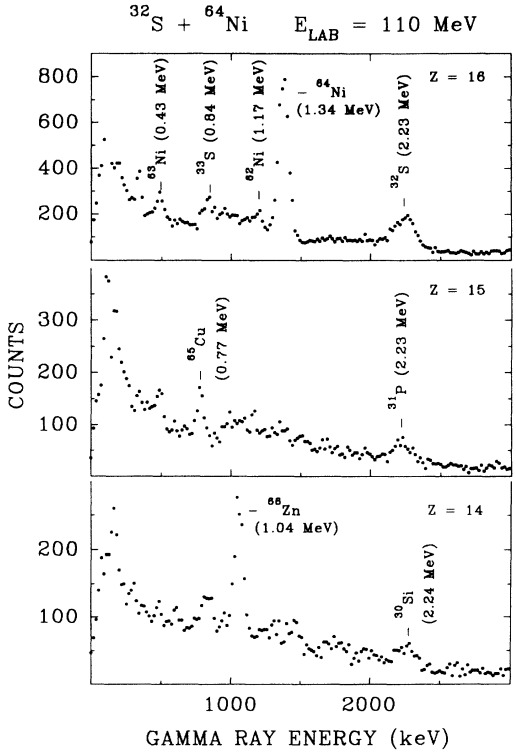

FIG. 3. Coincidence γ-ray spectra obtained by gating on $Z = 14$, 15, and 16 and integrated over the angular range of the heavy ion detector in the ^{32}S + ^{64}Ni system. The characteristic γ rays identified and used in the experiment are indicated.

the target and the projectile nuclei. The major γ rays from deexcitation of the levels populated in the one- and two-neutron pickup reactions can also be seen. The characteristic γ rays of the neutron stripping channels are not seen in the spectra. (ii) The γ spectra, in coincidence with $Z_P - 1$ and $Z_P - 2$ gates, showed mainly the γ rays from the nuclei obtained in one-proton and two-proton stripping channels ($-1p$ and $-2p$), respectively. The major γ transitions resulting from the $-1p1n$ and $-1p2n$ channels are found to be less than 25% of the yield of the major γ transition of the $-1p$ channel in both the systems studied. Stefanini *et al.* [21] measured the cross sections for up to four-nucleon transfer channels in ^{32}S + ^{64}Ni and did not report any yield of either of the $-1p1n$ and $-1p2n$ channels $\gtrsim$ 10% of the yield of the $-1p$ channel. The γ rays coming from the $-2p1n$ and the $-2p2n$ (or -1α) can also be identified. In ^{32}S + ^{64}Ni reactions, the relative yield of the 300 keV γ ray of ^{67}Zn resulting from $-2p1n$, compared to that of the 1040 keV γ ray of ^{66}Zn from $-2p$, was $\sim$ 5–10 %, and the relative yield of the 1780 keV ^{28}Si characteristic γ ray from $-2p2n$ (or -1α), compared to that of the 2235 keV ^{30}Si γ ray from $-2p$, was found to be about 50%. On the other hand, Stefanini *et al.* [21] found that the total $-2p1n$ and $-2p2n$ (or -1α) cross sections were $\sim$ 40% and 15%, respectively, of the $-2p$ cross section, indicating that the relative populations of the excited states and the ground states of the nuclei formed in the $-2p1n$ and $-2p2n$ channels are different. Thus, about 65% of the $Z_P - 2$ inclusive measured yield is due to two-proton stripping. (iii) There is a possibility that events observed in the $Z_P - 2$ band arise from one-proton stripping to states of high excitation energy ($\gtrsim$ 10 MeV) in $Z_P - 1$ nuclei, followed by single-proton evaporation. For these events, the Q value in the $Z_P - 2$ gated spectrum would be $Q < Q_{\text{g.s.}}$ $(-1p) - 10$ MeV, where $Q_{\text{g.s.}}$ is the ground state Q value. Most of the $Z_P - 2$ spectrum has higher energy or less negative Q value than this in the ^{28}Si + ^{68}Zn case, ruling out this possibility. Similar arguments apply to ^{32}S + ^{64}Ni also, even though not so strictly. Further, if the targetlike nucleus is excited in this process, the $Z_P - 2$ spectrum would be in coincidence with characteristic γ rays of the $Z_T + 1$ nucleus. These events were found to be $\lesssim$ 10% in both the systems studied.

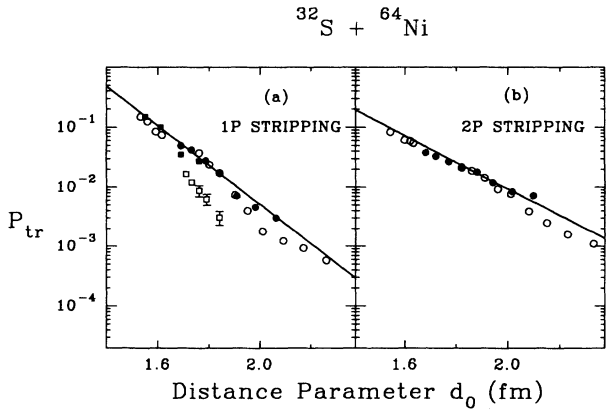

FIG. 4. Transfer probability plots for (a) $-1p$, (b) $-2p$ channels of the ^{32}S + ^{64}Ni system. The data points at 100 and 110 MeV bombarding energies are shown by open and solid circles, respectively. The solid lines are the least squares fit to all the data points. The $-1p$ transfer probabilities at $E_{\text{c.m.}}$ = 64.9 MeV and 54.2 MeV, estimated from Ref. [26], are shown by the open and the solid squares, respectively.

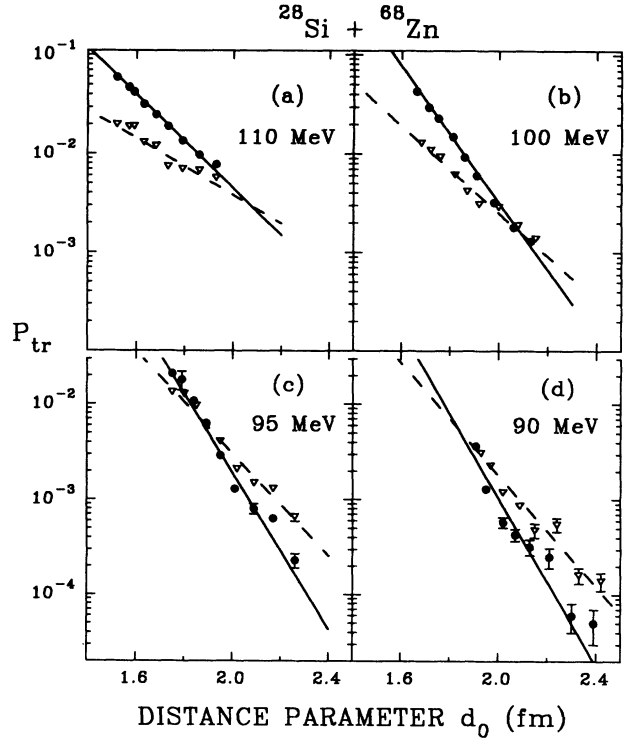

FIG. 5. One- and two-proton transfer probabilities, plotted as function of distance parameter d_0 at various bombarding energies in ^{28}Si + ^{68}Zn. The solid and the dashed lines are the fitted curves through $-1p$ (solid circles) and $-2p$ (open triangles) data points, respectively, for $d_0 \gtrsim 1.6$ fm.

The transfer probabilities P_{tr}, defined in Eq. (7) in Sec. III B, were obtained from the inclusive spectra and are plotted in Fig. 4 as function of the distance parameter $d_0 = r_0/(A_1^{1/3} + A_2^{1/3})$, where r_0 is the distance of closest approach [see Eq. (4) later; A_1 and A_2 are the masses of the interacting nuclei], for $-1p$ and $-2p$ channels in ^{32}S + ^{64}Ni at two energies. Similar plots for $-1p$ and $-2p$ channels in ^{28}Si + ^{68}Zn at four bombarding energies are shown separately in Fig. 5.

III. ANALYSIS

The results presented in the previous section were analyzed in terms of a semiclassical theory to describe the transfer reactions [16] and its influence on the measured fusion cross sections [7].

A. Semiclassical formalism

A semiclassical description of the heavy ion reactions in a coupled channels approach is given by Broglia and Winther [16]. In a first order perturbation approximation for such a theory, the amplitude for the colliding system to be in a channel β after the reaction ($t = \infty$) is given by

$$a_\beta(\infty) = \frac{1}{i\hbar} \int_{-\infty}^{\infty} F_\beta(r, Q_\beta)\, e^{i(Q_\beta - Q_{\rm opt})t/\hbar}\, dt, \qquad (1)$$

where $F_\beta(r, Q_\beta)$ is a form factor describing the transition from the incoming channel to the channel β, Q_β is the relevant Q value for the channel, and $Q_{\rm opt}$ is the optimum Q value, which is given from simple considerations [25] as

$$Q_{\rm opt} = \left(\frac{Z_P^f Z_T^f}{Z_P^i Z_T^i} - 1 \right) E_{\rm c.m.}, \qquad (2)$$

where i and f refer to the initial and final nuclei. The integral in Eq. (1) can be evaluated by considering the trajectory around the distance of closest approach, r_0, as given by

$$r(t) = r_0 + \tfrac{1}{2}\, \ddot{r}_0 t^2, \qquad (3)$$

where $\ddot{r}_0$ is the acceleration at r_0. The distance of closest approach is calculated for the entrance and the exit channels by assuming a Coulomb trajectory, using the relation

$$r_0 = \frac{Z_1 Z_2 e^2}{2(E_{\rm c.m.} + Q)} \left(1 + {\rm cosec}\, \frac{\theta_{\rm CM}}{2} \right) = d_0\, (A_1^{1/3} + A_2^{1/3}). \qquad (4)$$

Inclusion of nuclear potential modifies this relation for $d_0 \lesssim 1.6$ fm. Using the expression for the trajectory given by Eq. (3), the integral in Eq. (1) can be evaluated in a closed form with the result

$$a_\beta(\infty) = \frac{1}{i\hbar}\, F_\beta(r_0, Q_\beta) \sqrt{\frac{2\pi}{\alpha \ddot{r}_0}}\, \exp\left[-\frac{(Q_\beta - Q_{\rm opt})^2}{2\hbar^2 \alpha \ddot{r}_0} \right]. \qquad (5)$$

In obtaining this equation, the radial dependence of $F(r, Q)$ is taken as $F(r, Q) = F(r_0, Q)\, e^{-\alpha(r - r_0)}$. The transfer probability $P(r_0, Q_\beta) = |a_\beta(\infty)|^2$ is then given by the relation

$$P(r_0, Q_\beta) = \frac{\pi}{\sigma^2}\, |F_\beta(r_0, Q_\beta)|^2\, \exp\left[-\frac{(Q_\beta - Q_{\rm opt})^2}{2\sigma^2} \right], \qquad (6)$$

where $\sigma = \sqrt{\hbar^2 \alpha \ddot{r}_0 / 2}$. Equation (6) gives the probability of transfer to a given excited state β with Q value Q_β. From the Q-integrated transfer probability for each of the channels, the effective coupling strength F_0, taken as the average form factor at the barrier radius $r_0 = r_B$, was evaluated using Eq. (6).

B. Transfer probabilities

The Q-integrated transfer probability $P_{\rm tr}(r_0)$ is given by the expression

$$P_{\rm tr}(r_0) = \frac{\sigma_{\rm tr}}{\sigma_{\rm el} + \sigma_{\rm QE}}, \qquad (7)$$

where $\sigma_{\rm el}$, $\sigma_{\rm QE}$, and $\sigma_{\rm tr}$ are the differential cross sections for elastic, quasielastic, and the corresponding transfer channel, respectively. The transfer probability for each channel was obtained as the ratio of the respective measured yields, as the absolute cross sections were not determined. In case of a direct reaction, the trajectories at the entrance and the exit channels are different not only because of the Q value, but also because of the change in mass and charge as in a transfer reaction. For these transfer channels, the outgoing trajectories are smeared because of the spread in Q value. In other words, r_0 for the exit channel has a spread in addition to the shift due to difference in $Z_1 Z_2$ as in the case of charged particle transfer. The Q-integrated yield at a given $\theta_{\rm lab}$ is associated with the corresponding $P_{\rm tr}$ for an average distance of closest approach, which is the average of the distance of closest approach for the incoming channel and that for the outgoing channel corresponding to a Q value where the Q spectrum peaks (see Fig. 2). The spread in the Q values corresponds to a spread of $\pm 2\%$ in r_0 values for the cases studied in this experiment. Further, r_0 for the different transfer channels were found to be approximately within $\pm 3\%$ of the r_0 for the entrance channel.

As mentioned earlier, the measurements on the ^{32}S + ^{64}Ni system were done at $E_{\rm c.m.} = 66.7$ and 73.3 MeV which correspond to $E_{\rm c.m.}/V_B = 1.13$ and 1.24 (where V_B is the barrier height), while in ^{28}Si + ^{68}Zn system, they were made at $E_{\rm c.m.} = 58.8$, 63.7, 67.3, 70.8, 77.9, and 81.4 MeV with $E_{\rm c.m.}/V_B = 1.06$, 1.14, 1.21, 1.27, 1.40, and 1.46. According to Eq. (6), the transfer probability depends on the bombarding energy through the acceleration term $\ddot{r}_0$. The values of $\ddot{r}_0$ at $r_0 = 12$ fm vary only by factors of 1.6 and 1.2 for ^{28}Si + ^{68}Zn and ^{32}S + ^{64}Ni systems, respectively, in the studied energy ranges. Thus, one expects the probabilities to be almost independent of energy for the Q-value ranges measured and to fall on a common $P_{\rm tr}$ vs d_0 curve. This is approximately borne out for the ^{32}S + ^{64}Ni at the two energies and at the higher energies ($E_{\rm c.m.} = 77.9$ and 81.4 MeV) in ^{28}Si + ^{68}Zn. But as can be seen from the $P_{\rm tr}$ vs d_0 plots in Fig. 5 for ^{28}Si + ^{68}Zn, for a given d_0, the values of $P_{\rm tr}$ are lower at lower energies than at higher energies, especially for large d_0 values. Further, the variation of $P_{\rm tr}$ with d_0, characterized by α, also is seen to depend on the bombarding energy. The values of α vary from 0.3 to

0.7 fm^{-1} for $-1p$ and from 0.2 to 0.6 fm^{-1} for $-2p$ for the range of $E_{\rm c.m.}/V_B = 1.5$–1.1 as shown in Fig. 6. The situation is similar in the case of the ^{32}S + ^{64}Ni system, if we combine the present data with that of Napoli *et al.* [26], who measured $-1p$ and $+1n$ transfer reactions around V_B. While the higher energy ($E_{\rm c.m.} = 64.9$ MeV) data of Napoli *et al.* for the $-1p$ channel is consistent with our data as can be seen from Fig. 4(a), the value of $P_{\rm tr}$ deduced from their measurements at $E_{\rm c.m.} = 54$ MeV is lower than those at higher energies. The slope parameter α is also larger at lower energy than in our measurements. Thus a common feature observed in both the systems is an apparent dependence of the slope parameter α on the bombarding energy, a feature which is not expected on the basis of semiclassical theory.

In the semiclassical theory, α depends on the binding energy E_B of the transferred particle of reduced mass μ in the target or the projectile nuclei through the relation $\alpha = \sqrt{2\mu E_B}/\hbar$. If one considers an average for the target and the projectile and corrects the binding energies for the Coulomb potential in the case of proton transfers, one can write [12]

$$\alpha = \frac{1}{2}\left[\alpha_p\sqrt{1-\frac{0.5E_x}{E_B^P}} + \alpha_T\sqrt{1-\frac{0.5E_x}{E_B^T}}\right], \qquad (8)$$

where $E_B^{P(T)}$ are the effective binding energies for the transferred particle in the projectile (target) nuclei, and E_x is the mean excitation energy for the proton transfer channel. The average α's estimated in this way for one- and two-proton stripping in ^{28}Si + ^{68}Zn are $\alpha_{1p} \approx 0.78$ fm^{-1} and $\alpha_{2p} \approx 1.52$ fm^{-1}, respectively, consistent with the relation between the slopes as $\alpha_{2p} \approx 2\alpha_{1p}$. This is expected if the two-proton transfer is considered as a sequential process so that the relation between the probabilities becomes $P_{2p} \sim P_{1p}^2$. Even a correlated two-nucleon transfer is expected to result in $\alpha_{2p} \approx 2\alpha_{1p}$, since the two nucleon binding energy is not very different from twice that of one nucleon (the pairing energy is small compared to $2E_B$) and the mass of the correlated pair is twice that of one nucleon. It can be seen from Fig. 6 that while α_{1p} approaches the estimated value (shown by the dashed line in the figure) at energies below $1.2V_B$, α_{2p} still shows an increasing trend towards the value predicted by semiclassical theory (shown by the dotted line in the figure), attaining a value which is approximately half of the expected value at the barrier. A "hot" transfer, in which the transfer takes place to highly excited states where the particles are very loosely bound, can result in smaller slope parameters. Such an explanation for the observed smallness of α_{2p} is not likely to be valid since the observed slope does not show a marked dependence on the Q value.

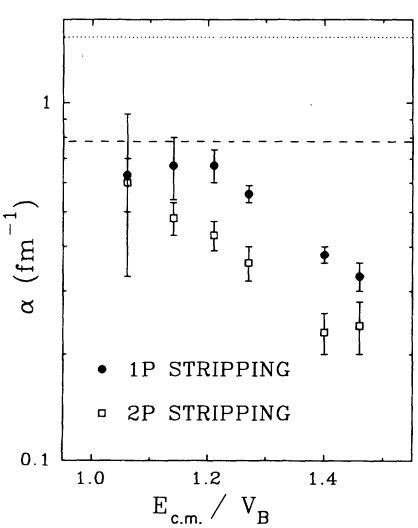

FIG. 6. Effective slope parameters α in one- and two-proton stripping, plotted as function of $E_{\rm c.m.}/V_B$ in ^{28}Si + ^{68}Zn. The dashed and the dotted lines are the expected values of α_{1p} and α_{2p} from the semiclassical theory.

In the semiclassical picture, the width of the Q-value distribution is related to the slope parameter α as $\sigma = \sqrt{\hbar^2\bar{r}_0\alpha/2}$, and can be calculated to be $\sigma_{1p} \approx 2.7$ MeV and $\sigma_{2p} \approx 3.7$ MeV in the ^{28}Si + ^{68}Zn system at 110 MeV, if the expected values of the slope parameters are used. The observed values of the widths are 2.8 MeV and 4.2 MeV, respectively, and do not have a marked dependence on the bombarding energy. The slope parameters α, on the other hand, have an unexpectedly large dependence on the bombarding energy.

Slope anomalies have been observed earlier in several cases [13]. Recently, Wuosmaa *et al.* [17] and Liang *et al.* [18] observed such anomalies for two-neutron and two-proton transfers, respectively, in ^{32,36}S + ^{92,98,100}Mo systems for energies just above the barrier. In the energy regions studied, they do not observe an anomaly for the one-nucleon transfer reactions. The present results also show similar features for two-proton stripping in the ^{28}Si + ^{68}Zn system. In addition, even the one-proton stripping shows anomalous behavior for $E_{\rm c.m.}/V_B \gtrsim 1.3$. The authors of Refs. [17,18] attribute the slope anomaly to inapplicability of the semiclassical theory arising out of localization in angular momentum space. Vigezzi and Winther [27] pointed out that for angles less than the Coulomb rainbow angle, more than one impact parameter can contribute. They also showed that for such angles, the contribution from the so-called "nuclear branch," while not so important for elastic scattering, becomes very important for transfer reactions. Baba and Schindler [28] analyzed the above-mentioned cases of slope anomaly and conclude that they can be understood in terms of the nuclear branch.

C. Effect on the sub-barrier fusion enhancement

The $P_{\rm tr}$ vs d_0 plots shown in the Figs. 4 and 5 are fitted by the exponential function

$$P_{\rm tr}(r_0) = P_{\rm tr}(r_B)\,\exp\,[-2\alpha(r_0 - r_B)] \qquad (9)$$

to obtain $P_{\rm tr}(r_B)$, the transfer probability at the barrier radius r_B, and the slope parameter α. In the case of ^{28}Si

+ ^{68}Zn, the higher energy data (115–100 MeV) were used for this purpose.

The effective coupling strengths of the $-1p$ and $-2p$ channels, evaluated from Eq. (6) and the Q-value spectra, are used to estimate the role of these transfer channels on the sub-barrier fusion enhancement using the simplified coupled channels formalism of Dasso *et al.* [29] incorporated in the code CCFUS. In this formalism, the form factors and the Q values of different inelastic excitation and transfer channels are given as input. In case of the even-even nuclei considered in this experiment, the 2^+ and 3^- vibrational states in both the colliding nuclei were included as inelastic channels. The corresponding form factors used in the calculations were discussed in Ref. [19].

The Q-value distributions and their effect on the coupling strengths that go into these calculations were taken into account by binning the Q spectra for $Q_{\text{g.s.}} \lesssim Q \lesssim (Q_{\text{g.s.}} - 5)$ MeV and appropriately weighing the strengths by the Q-value spread of the respective bins.

From the experimental fusion cross sections, taken from Refs. [19,20] for the ^{32}S + ^{64}Ni system, the observed barrier shift D_0 is ~ 3.5 MeV, of which ~ 1.4 MeV can be accounted for by the inelastic couplings. Inclusion of $-1p$ and $-2p$ channels contributes only another ~ 0.3 MeV to the D_0 which clearly indicates the need to include the neutron transfer channels. Of these channels, the $+2n$ channel with positive $Q_{\text{g.s.}}$ is expected to be more important in this respect [29]. From the experimental fusion cross section data on the ^{28}Si + ^{68}Zn system, taken from Ref. [19], the observed barrier shift is 2.6 MeV, of which an about 1.6 MeV barrier shift can be accounted for by the inclusion of inelastic couplings alone. The $-1p$ and $-2p$ couplings contribute an additional ~ 0.2 MeV to D_0, clearly indicating the need to include the neutron transfer channels. The important difference noticed in this regard between the two systems is that while the inelastic couplings account for almost 60% of the barrier shift in the ^{28}Si + ^{68}Zn, it can account only for about 40% shift in the case of ^{32}S + ^{64}Ni. Thus, it is likely that coupling of the neutron transfer channels is more important in ^{32}S + ^{64}Ni, possibly because of the more positive $Q_{\text{g.s.}}$ and/or significant coupling strength for the $+2n$ channel.

IV. SUMMARY AND DISCUSSION

The one- and two-proton transfer probabilities in ^{32}S + ^{64}Ni and ^{28}Si + ^{68}Zn were measured at several energies near the Coulomb barrier. The latter system was studied for energies ranging from $E_{\text{c.m.}}/V_B = 1.1$–$1.5$. The effective slope parameter for the one-proton stripping reaction varies from 0.7 to 0.3 fm^{-1} over the above energy range, as compared to a value of ~ 0.8 fm^{-1} estimated on the basis of semiclassical theory. The slope parameter for two-proton stripping varies from 0.6 to 0.2 fm^{-1} over that range in contrast to a semiclassical prediction of 1.5 fm^{-1}.

The effective coupling strengths for each of these proton transfer channels were obtained from the measured transfer probabilities using a semiclassical theory. These were then used in the simplified coupled channels calculations program CCFUS to calculate the fusion cross sections at energies below and above the barrier. The results of these calculations in both the systems studied clearly show that inclusion of the one- and two-proton stripping channels alone does not explain the enhancement of the sub-barrier fusion cross section, despite significant coupling strengths for these channels, indicating the importance of the one- and two-neutron pickup channels in explaining the sub-barrier fusion enhancement. Therefore, it is important to study the neutron transfer reactions for these systems studied here.

ACKNOWLEDGMENTS

The authors would like to thank M.D. Deshpande for developing the gas detector system used in this experiment and D.C. Ephraim for preparing the enriched targets with great care. We also thank M.K. Sharan, S. Chattopadhyay, S.D. Paul, and F. Sutaria for their help in taking data and A. Navin for doing some of the coupled channels calculations.

[1] *Proceedings of Workshop on Heavy Ion Collisions at Energies Near the Coulomb Barrier*, Daresbury, U.K., 1990, edited by M.A. Nagarajan (Institute of Physics Press, New York, 1991).
[2] G.R. Satchler, M.A. Nagarajan, J.S. Lilley, and I.J. Thompson, Ann. Phys. (N.Y.) **178**, 110 (1987).
[3] A.K. Mohanty, S.V.S. Sastry, S.K. Kataria, and V.S. Ramamurthy, Phys. Rev. Lett. **65**, 1096 (1990).
[4] T. Udagawa and T. Tamura, Phys. Rev. C **29**, 1922 (1984).
[5] P.H. Stelson, Phys. Lett. B **205**, 190 (1988).
[6] C.E. Aguiar, L.F. Canto, and R. Donangelo, Phys. Rev. C **31**, 1969 (1985).
[7] C.H. Dasso, S. Landowne, and A. Winther, Nucl. Phys. **A432**, 495 (1985), and references therein.
[8] C.H. Dasso and S. Landowne, Comput. Phys. Commun. **46**, 187 (1987).
[9] K.E. Rehm, F.L.H. Wolfs, A.M. van den Berg, and W. Henning, Phys. Rev. Lett. **55**, 280 (1985).
[10] A.M. Stefanini *et al.*, Nucl. Phys. **A456**, 509 (1986).
[11] R.A. Broglia, G. Pollarolo, and A. Winther, Nucl. Phys. **A361**, 307 (1981).
[12] L. Corradi *et al.*, Z. Phys. A **335**, 55 (1990).
[13] C.Y. Wu, W. von Oertzen, D. Cline, and M.W. Guidry, Annu. Rev. Nucl. Part. Sci. **40**, 285 (1990).
[14] K.E. Rehm, Annu. Rev. Nucl. Part. Sci. **41**, 429 (1991).
[15] G. Bertsch and R. Schaeffer, Nucl. Phys. **A277**, 509 (1977).

[16] R.A. Broglia and A. Winther, *Heavy Ion Reactions Lecture Notes* (Addison-Wesley, Redwood City, CA, 1991), Vol. I.
[17] A.H. Wuosmaa, K.E. Rehm, B.G. Glagola, Th. Happ, W. Kutschera, and F.L.H. Wolfs, Phys. Lett. B **255**, 316 (1991).
[18] J.F. Liang, L.L. Lee, Jr., J.C. Mahon, and R.J. Vojtech, Phys. Rev. C **47**, R1342 (1993).
[19] M. Dasgupta, A. Navin, Y.K. Agarwal, C.V.K. Baba, H.C. Jain, M.L. Jhingan, and A. Roy, Nucl. Phys. **A539**, 351 (1992).
[20] R.J. Tighe, J.J. Vega, E. Aguilera, G.B. Liu, A. Morsad, J.J. Kolata, S.H. Fricke, H. Esbensen, and S. Landowne, Phys. Rev. C **42**, 1530 (1990).
[21] A.M. Stefanini *et al.*, Phys. Lett. B **185**, 15 (1987).
[22] M. Rhoades-Brown, S. Pieper, and M. Macfarlane, coupled channels version of PTOLEMY, ANL report, 1980 (unpublished).
[23] S. Saha, Y.K. Agarwal, M.D. Deshpande, and A. Roy, Nucl. Instrum. Methods A **335**, 165 (1993).
[24] M. Jääskeläinen, D.G. Sarantites, R. Woodward, F.A. Dilmanian, J.T. Wood, R. Jääskeläinen, D.C. Hensley, M.L. Halbert, and J.H. Barker, Nucl. Instrum. Methods **204**, 385 (1983).
[25] R. Bass, *Nuclear Reactions with Heavy Ions*, Texts and Monographs in Physics (Springer-Verlag, Berlin, 1980).
[26] D.R. Napoli *et al.*, Nucl. Phys. **A559**, 443 (1993).
[27] E. Vigezzi and A. Winther, Ann. Phys. (N.Y.) **192**, 432 (1989).
[28] C.V.K. Baba and F. Schindler (unpublished).
[29] C.H. Dasso, S. Landowne, and A. Winther, Nucl. Phys. **A405**, 381 (1983).

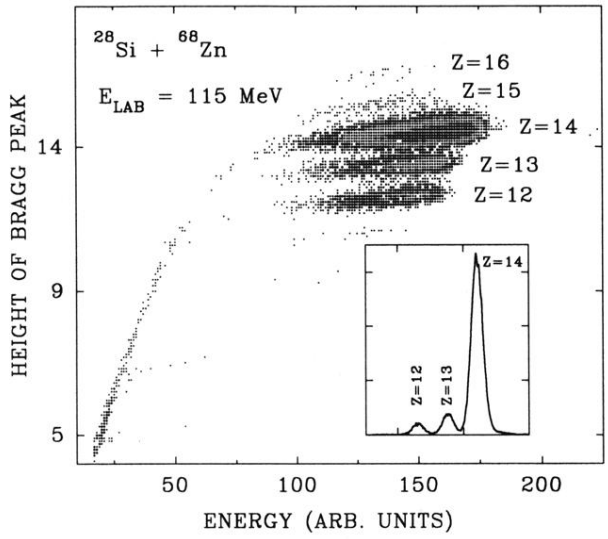

FIG. 1. Two-dimensional plot of Z and E of the ions integrated over the observed angular range in ^{28}Si + ^{68}Zn. Small yields of $Z = 15$ and $Z = 16$ can be seen but were not analyzed. Inset shows E gated Z spectrum.